

Momentum Distribution in Solar Flare Processes

H.S. Hudson · L. Fletcher · G.H. Fisher · W.P. Abbett ·
A. Russell

Received: 29 December 2010 / Accepted: 4 July 2011 / Published online: 4 October 2011
© Springer Science+Business Media B.V. 2011

Abstract We discuss the consequences of momentum conservation in processes related to solar flares and coronal mass ejections (CMEs), in particular describing the relative importance of vertical impulses that could contribute to the excitation of seismic waves (“sunquakes”). The initial impulse associated with the primary flare energy transport in the impulsive phase contains sufficient momentum, as do the impulses associated with the acceleration of the evaporation flow (the chromospheric shock) or the CME itself. We note that the deceleration of the evaporative flow, as coronal closed fields arrest it, will tend to produce an opposite impulse, reducing the energy coupling into the interior. The actual mechanism of the coupling remains unclear at present.

Keywords Solar flare

1. Introduction

The conservation of linear momentum has not often been considered in discussions of the dynamics of solar flares and coronal mass ejections (CMEs). The exception to this is in the evaporative flow, where several authors have described the theoretical (Brown and Craig, 1984; McClymont and Canfield, 1984) and observational (Zarro *et al.*, 1988; Canfield *et al.*, 1990) consequences: redshifts must occur to compensate for blueshifts as the chromosphere expands. Indeed, recent spectroscopic observations have shown an interesting temperature dependence of these red and blue shifts (*e.g.*, Milligan and Dennis, 2009), with a division at about 2×10^6 K.

Solar Flare Magnetic Fields and Plasmas
Guest Editors: Y. Fan and G.H. Fisher

H.S. Hudson (✉) · G.H. Fisher · W.P. Abbett
SSL/University of California, Berkeley, CA, USA
e-mail: hudson@ssl.berkeley.edu

H.S. Hudson · L. Fletcher · A. Russell
School of Physics and Astronomy, SUPA, University of Glasgow, Glasgow G12 8QQ, UK

In this article we qualitatively explore the consequences of momentum conservation in other aspects of solar flares. These include not only the momentum associated with the bodily transfer of mass, as with the evaporative flow and with CMEs, but also that represented by significant wave transport of energy (*e.g.*, Fletcher and Hudson, 2008; Haerendel, 2009). In fact, the low plasma β of the corona (*e.g.*, Gary, 2001) means that the momentum will reside mostly in the electromagnetic field, rather than in the matter. Energy transport *via* the Alfvénic Poynting flux (for a discussion in the context of magnetic-reconnection flare models see Birn *et al.*, 2009) must happen if a flare represents the release and redistribution of coronal energy storage, and its dissipation as chromospheric radiation.

Quantitative estimates of the impulse in the energy-release phase depend on our knowledge of the coronal magnetic field and the exact nature of its restructuring, and the skimpiness of this knowledge probably accounts for the lack of prior work on this subject. Solar flares occur in a complicated magnetized plasma environment often described in the approximation of ideal MHD. In principle, MHD simulations can explore the properties of momentum in flares and CMEs, but in practice this aspect of the physics is not emphasized. Simple arguments based on body forces acting on discrete objects (where does one push on a CME exactly?) generally are of less value than descriptions of the hydrodynamic aspects of the flows (see the description by Fisher *et al.*, 2011). Note that flare plasmas involve substantial particle acceleration that also must be included in momentum assessments (Brown and Craig, 1984; McClymont and Canfield, 1984). This aspect of the momentum balance would not be a part of any ideal MHD theory or simulation.

To a good approximation, a flare–CME occurs in a stationary solar atmosphere with zero net momentum. At the end of the process, if no CME has happened, another similar stationary state will result, although mass and energy will have been redistributed. If a CME does happen, mass and waves flow into the solar wind and are lost to the Sun forever, and this will also result in a displacement and a small change of the momentum of the body of the Sun. Here “small” can be put in the context that $\Delta v_{\odot} = m_{\text{CME}}/M_{\odot} \times v_{\text{CME}}$, of order $10^{-10} \text{ cm s}^{-1}$. This is doubtless entirely irrelevant for a solar-type star.

Flare seismic signatures in the solar interior (“sunquakes”: Kosovichev and Zharkova, 1998) require momentum acquired from the coronal–chromospheric dynamics of a flare (Wolff, 1972). Zharkova and Zharkov (2007) and Zharkova (2008) discuss this problem in detail via analyses of the flares SOL1996-07-09T09:11 and SOL2003-10-28T11:10. Various mechanisms have been invoked to relate the seismic waves to the flare processes themselves, and the observations point to the flare footpoints during the impulsive phase (Kosovichev and Zharkova, 1998; Donea and Lindsey, 2005) as the seismic sources. Another characteristic of the impulsive phase is the evaporation flow that fills the coronal flare loops with hot plasma, creating the coronal X-ray sources. We point out (Section 2.2) that evaporation into closed fields implies a pair of impulses – a first impulse to accelerate the mass up into the corona, and a second and opposite one to arrest its motion there. We discuss the implications of this characteristic for seismic waves specifically in Section 3.

2. Application of Linear Momentum Conservation

2.1. Reference Flare Parameters

This article discusses momentum conservation in flares and CMEs. We only consider the vertical component of linear momentum. For a concrete context we consider a typical X1-class solar flare with a CME, and assume the parameters listed in Table 1. At this flare

Table 1 Representative parameters for an X-class flare with CME and sunquake.

Property	Value
Total energy of flare	10^{32} erg
Flare-loop height	1×10^9 cm
Coronal density (preflare)	1×10^9 cm $^{-3}$
Coronal field	1×10^3 G
Impulsive sub-burst duration	10 s
Impulsive-phase duration	100 s
Number of sub-bursts	10
Impulsive sub-burst footpoint area	3×10^{17} cm 2
Evaporation speed	5×10^7 cm s $^{-1}$
Evaporated mass	1×10^{14} g
Draining time	1000 s
CME mass	1×10^{15} g
CME speed	2×10^8 cm s $^{-1}$
Seismic-wave energy ^a	4×10^{27} erg

^a Moradi *et al.* (2007).

magnitude, a CME is likely but sometimes does not happen; for less energetic flares, CME occurrence becomes less probable (Yashiro *et al.*, 2005; Wang and Zhang, 2007). Section 2.4 discusses the case of a flare with no CME.

As a guide to representative parameters of a flare–CME system, we assume that the flare impulsive phase consists of a series of ten independent impulsive sub-bursts as indicated in Table 1; this is just illustrative since a broad distribution of time scales for sub-bursts exists, ranging down to time scales below one second (Kiplinger *et al.*, 1984). The conceptual flare also involves a seismic wave (sunquake) containing 4×10^{27} erg, taken as 0.01% of the total flare energy (Moradi *et al.*, 2007). The information in Table 1 is meant to be representative and is certainly incomplete in the sense that it omits various features. We include the seismic wave because of its interesting diagnostic relationship to momentum conservation.

In the scheme considered (Figure 1), energy originates in the corona and flows into the flare footpoints either as in the standard thick-target model of an electron beam, or via Alfvénic Poynting flux (Fletcher and Hudson, 2008). The energy released in the footpoints drives the evaporative flow, which is arrested in an arcade of magnetic field and eventually drains back into the chromosphere. The complementary momentum for the evaporation flow appears in a downward wave structure in the deeper atmosphere (Kostiuk and Pikel'ner, 1975). From one equilibrium state to the next, this scheme involves four major impulse pairs with balanced vertical momentum components: the impulse associated with the primary energy release in the corona (*a–a* in Figure 1), that involved in the chromospheric heating and evaporation (*b–b*), that associated with the arrested evaporative flow (*c–c*), and (for completeness) that associated with the drained material (*d–d*) impacting the chromosphere (Hyder, 1967). The balancing impulses may be separated in time via transport of energy and momentum through the plasma by flows, waves, or particles. The flare results from that portion of the primary energy release carried into the lower solar atmosphere.

2.1.1. Beams

In the generally accepted picture, the energy of a flare comes from magnetic energy storage in the strong magnetic fields of an active region, on a characteristic scale of 10^9 cm (here

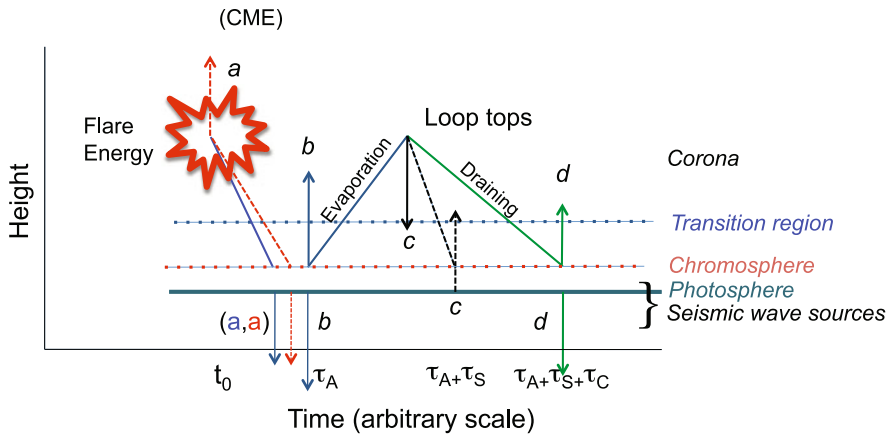


Figure 1 Timeline of the vertical impulses in an idealized solar flare with (optional) CME. The temporal axis is nonlinear and highly schematic in this representation. The initial primary energy release (the flare) communicates an impulse to the chromosphere on a time scale τ_a , reflecting either the beam propagation time (if particles convey the energy) or the Alfvén transport time (if waves). In either case this time scale is smaller than the evaporation time scale τ_s , which itself is shorter than the draining time scale τ_c . The impulsive-phase transport has two alternatives: the classical electron beam and the Poynting-flux alternative of Fletcher and Hudson (2008). The solid lines and arrows show energy transport and impulses in matter, and the dashed lines and arrows show the same in waves. The impulse pairs are labeled by letters, *i.e.* the pair *a–a* shows the pair related to primary energy release, *b–b* that associated with the flare heating itself, *etc.*

we restrict ourselves to events occurring in active regions). Timing evidence suggests that for CMEs associated with active-region flares, their energy too derives from a similar source (Dere *et al.*, 1997; Zarro *et al.*, 1999; Zhang *et al.*, 2004; Temmer *et al.*, 2008).

On the other hand, the radiated energy of a flare comes mainly from the chromosphere and photosphere (*e.g.*, Emslie *et al.*, 2005), and a substantial (if not dominant) part of this energy appears in the impulsive phase of the flare (here taken to be the rise phase of the GOES soft X-ray burst accompanying the flare). This means that the energy must propagate from its coronal storage region into the chromosphere on a relatively short time scale. The standard thick-target model (*e.g.*, Brown, 1971; Kane and Donnelly, 1971; Hudson, 1972) assigns this propagation to a beam of non-thermal electrons (see Section 2.1.2 for the Poynting-flux alternative). Variants of the thick-target model with protons (Najita and Orrall, 1970; Švestka, 1970) or neutral beams (Simnett and Haines, 1993) have also been proposed; these would contain larger momenta than the electron beams.

The vertical momentum transport by an electron beam in the thick-target model can be estimated from the observed hard X-ray flux (Brown and Craig, 1984; McClymont and Canfield, 1984). We can estimate the total momentum of the beam as $p = Nm_e v_e$, where v_e is the mean vertical electron speed and N the total number of electrons. This omits several complicating factors, including the return current (Knight and Sturrock, 1977) required by the charge-neutrality condition, which could substantially reduce the momentum contained in the beam. Nevertheless if we generalize the model geometrically by allowing a curved flux tube, then the beam (and its anti-beam) will drive impulses (of the same sign) into the field (Section 2.1.2), in which case our simple estimate is of the right order of magnitude.

For a concrete example (one ten-second sub-burst) we take $E = 10^{31}$ erg and $v_e = 10^{10}$ cm s⁻¹ for a momentum $p = 2 \times 10^{21}$ gm cm s⁻¹. The impulse imparted to the photosphere over an area A and time Δt corresponds to a beam pressure $P = p/A\Delta t =$

6×10^2 dyne cm^{-2} for beam area 3×10^{17} cm^2 and ten-second duration. Smaller times or areas would result in larger beam pressures. This illustrative number, based on TRACE and *Hinode* white-light flare observations (Hudson, Wolfson, and Metcalf, 2006; Fletcher *et al.*, 2007; Isobe *et al.*, 2007), makes an important point: the beam dynamic pressure exceeds the pressure of the ambient atmosphere, even in semi-empirical models of flare atmospheres such as the FLB model of Mauas, Machado, and Avrett (1990). In this flare model the pressure at $n = 10^{13}$ cm^{-3} is only about 20 dyne cm^{-2} . Brown and Craig (1984) also make this point about the radiative-transfer models, and McClymont and Canfield (1984) note that the hydrodynamic pressures due to heating and evaporation should be much greater in magnitude.

We conclude that the existing semi-empirical models of the lower atmosphere during a flare probably do not represent the impulsive phase well.

2.1.2. Waves

Energy transport via Alfvén waves at low plasma β implies a momentum flux S/v_A , where S is the (Alfvénic) Poynting flux, and v_A the Alfvén speed. This momentum flux, and the time scales of the reaction in the photosphere, are similar to those expected in the thick-target model. The high speeds of particles or Alfvén waves mean that only a small temporal interval separates the energy-release time in the low corona from the impulse applied to the Sun. This initial impulse begins to appear where the energy is absorbed; for the thick-target model this is normally calculated from the electron deflections by Coulomb scattering (Brown, 1971). In the case of wave transport, it depends upon the mechanism for wave damping, but this may ultimately be in the form of similar electron distributions (Fletcher and Hudson, 2008).

The Alfvén speed can be quite high in the core of an active region: 1000 G and $n_e = 10^9$ cm^{-3} corresponds to $v_A/c \approx 0.3$. Figure 2 (left) compares the ion sound speed with the Alfvén speed for Model 1006 (sunspot umbra) of Fontenla *et al.* (2009). Figure 2 (right) illustrates the slowing-down of an Alfvénic wave packet as it passes through the photosphere, using the same model. We have assumed a uniform magnetic field of 3000 G for this estimate, which leads to an elapsed time of 38 seconds between the top of the model and its base. At the base of this model atmosphere (164 km below $\tau_{5000} = 1$) the sound speed increases with depth, and energy deposited in this region can enter the interior and be trapped there as a sunquake. Fisher *et al.* (2011) discuss the theory of this coupling.

The case shown in Figure 2 is for a reasonable assumption about the magnetic field at the umbral photosphere. For the Poynting-flux model of the impulsive-phase energy transport (Fletcher and Hudson, 2008) we could interpret this roughly as the time delay between the hard X-ray burst and the injection time of acoustic energy into the interior. In principle, this delay would be different for particle or wave transport, and for direct photospheric heating via radiative backwarming (Machado, Emslie, and Avrett, 1989). Kosovichev (2007) discusses the complications resulting from multiple acoustic sources that may compete in a given flare event. In general, the timing delay seen in Figure 2 also suggests a filtering effect as regards sunquake amplitude, because it spreads the energy out temporally. For the case shown, the total delay $\tau \approx 38$ seconds would correspond to a wave frequency $f = (2\pi\tau)^{-1} \approx 5$ mHz, near the frequency band often used for sunquake studies, and the observations would not capture some fraction of the high-frequency power.

2.2. Evaporation

The evaporative flow presents a complicated set of momentum issues. The energy from the corona, by whatever means, heats the chromosphere impulsively and drives matter up

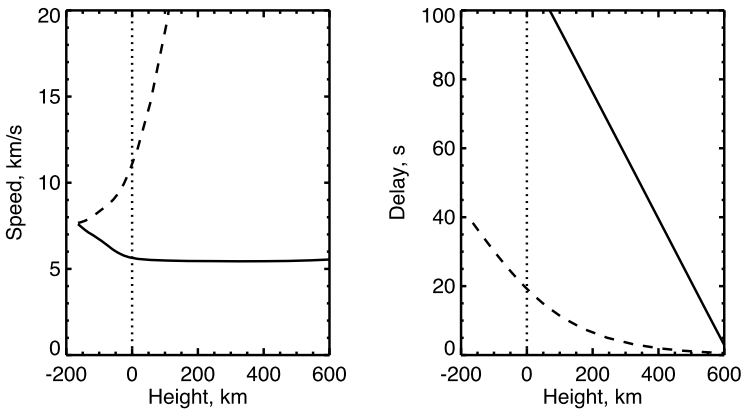


Figure 2 Left: sound- (solid) and Alfvén-speeds for the Fontenla *et al.* (2009) model atmosphere for a sunspot umbra (their Model 1006), assuming a magnetic field of 3000 G. Right: time elapsed for energy to arrive from the corona. The solid line shows the acoustic travel time, and the dashed line the Alfvénic.

and down. Momentum is conserved, and that of the upward mass flux (and waves) must be compensated by downward momentum. The upward flow is the chromospheric evaporation, and the downward flow converts into a shock wave that dissipates radiatively (Fisher *et al.*, 2011). This is the hydrodynamic response initially described by Kostjuk and Pikel’ner (1975). The momentum balance of the initial expansion can be observed via bisector analysis of chromospheric lines (Zarro *et al.*, 1988; Canfield *et al.*, 1990). The downward component eventually appears, as described, as a miniscule acceleration of the Sun, and some of its energy may excite sunquake acoustic waves (see Section 3) as envisioned by Kosovichev and Zharkova (1998).

The evaporated mass flows up into closed loops on relatively short time scales; at the loop top the vertical flow is arrested by the magnetic field, which provides the necessary impulse. This second (magnetic) impulse acts on the body of the Sun via wave coupling that we do not consider here; the general effect would be to launch a bipolar wave front (*i.e.*, two successive perturbations of opposite sign) into the solar interior. The second impulse would be spread out over a longer time scale owing to the dispersion of the evaporated mass as it flows up into the flux tube. The transfer of momentum into the photosphere will also be dispersed because of the wave propagation. Figure 1 sketches how the complete impulse might appear for a single ten-second pulse. This compensating impulse from the stoppage of the evaporation flow could presumably be exerted at the footpoints corresponding to the initial evaporation flow, or it could be spread more widely depending on the details of the wave transport of the momentum. The complicated properties of the momentum transfer associated with the presence of closed fields presumably will require analysis via numerical simulation, and we do not think that the standard 1D radiation hydrodynamics can capture the necessary physics since it omits the Lorentz force.

2.3. CMEs

Momentum balance in the CME ejection depends upon the time scale of the acceleration of the mass, plus unknown magnetic effects. The magnetic effects, as discussed above, must dominate initially if the energy source is in the low- β coronal field, but the momentum can appear ultimately in the mass flow swept up by the ejection; according to Table 1 the

Table 2 Vertical momentum components, representative X-class flare with CME.

Item	Phenomenon	Mass	v	Δt	Momentum	Pressure
Figure 1		g	km s ⁻¹	s	g cm s ⁻¹	dyne cm ⁻²
a	Primary (e ⁻) ^a	2×10^{11}	$c/3$	10	2×10^{21}	7×10^2
a	Primary (p ⁺ or H) ^a	1×10^{13}	2×10^8	10	1×10^{23}	3×10^5
a'	Primary (waves)	–	$c/3$	10	1×10^{21}	3×10^2
b	Evaporation flow	10^{14}	500	10	2×10^{22}	2×10^3
b'	Radiation ^b	–	c	10	1×10^{19}	3
c	CME	10^{15}	2000	100	2×10^{23}	?
d	Draining	10^{15}	10	$\approx 10^4$	2×10^{21}	0.07
	Seismic wave ^c				8×10^{21}	

^a20 keV if e⁻, 20 MeV if p⁺ or H.

^bWhite-light flare.

^cKosovichev and Zharkova (1998), adjusted to X1.

observed CME momentum is consistent with this idea. The total magnitude of the mass component of CME momentum, for a major CME of 10^{15} g at a speed of 2×10^3 km s⁻¹ is 2×10^{23} g cm s⁻¹. The source of the CME mass and its acceleration cannot be determined very completely from coronagraphic observations, owing to the presence of the occulting edge, and generally must be described in terms of non-coronagraphic observations in X-rays or at other wavelengths (*e.g.*, Hudson and Cliver, 2001). Observations of X-ray dimming (Hudson and Webb, 1997) and coronagraphic height-*vs.*-time plots (Zhang *et al.*, 2004; Temmer *et al.*, 2008) clearly point to the impulsive phase of the flare for flare-associated CMEs. However, the data are not good enough to determine the properties of the acceleration on the fine time scales of the impulsive-phase variations. The mass of a CME also includes (and may be dominated by) the mass swept up from the corona itself during the eruption, but on time scales much longer than those of the impulsive phase. Moreover the footprint in the photosphere of the magnetic structures involved in CME formation is not understood in detail, and so we generally only have upper limits on the spatial and temporal scales of the impulse imparted to the photosphere. Hence Table 2 has no entry for the pressure that the CME produces in the lower atmosphere.

2.4. No CMEs

In general a flare does not have an accompanying CME, even for some X-class events (Wang and Zhang, 2007). In such a case, how can momentum be conserved in the initial energy release? We can only speculate about this, since there do not appear to be any relevant observations. We suggest that the upward impulse, needed to balance the downward push on the photosphere, takes the form of waves radiated upwards and not damped in the mass flow of the CME. In this situation the plasma has no bulk flow and the waves propagate relatively freely through the nearly stationary medium, without rapid damping (Axford and McKenzie, 1992). As described by Belcher (1971), the wave energy can eventually exert substantial pressure on the solar wind as the waves damp. Because we rarely see type II radio bursts in the absence of CMEs (but see Klein, Trotter, and Klassen, 2010 for a good example of one), we suspect that the magnetic-pressure pulse may be generally more gradual than a

gas-pressure pulse would be, because of weak damping. This would presumably soften the wave front and delay the “ignition” of the type II emission because the shock condition would not be met so readily (*e.g.*, Vršnak and Lulić, 2000).

2.5. Summary

Figure 1 schematically summarizes the momentum transport in a flare–CME. The impulse associated with flare energy release in the corona, and delivered downwards, must appear ultimately in the photosphere. The recoil takes the form of the sunquake waves. The upward impulse may escape into the solar wind if a CME occurs, but the theory remains to be worked out. The stepwise changes observed in the photospheric field presumably are involved in the momentum transfer, but this will not be known quantitatively until these changes can be observed in the vector field. The propagation of the force between the corona and the photosphere presumably involves Alfvénic wave packets (Song and Lysak, 1994) with general motions of the plasma, including both tension and pressure forces. The waves may include non-MHD properties as well. We summarize the estimated momentum values in Table 2, which uses the representative flare parameters given in Table 1.

3. Seismic Waves

Flare-related seismic waves were first observed by Kosovichev and Zharkova (1998) following the prediction by Wolff (1972). Wolff also described the momentum transfer that we discuss here, and also the excitation of the p -mode standing waves. Observations have shown that the “sunquake” seismic waves originate in the impulsive phase, specifically the locations of the white-light flare, the magnetic transients, and the hard X-ray footpoints (Kosovichev and Zharkova, 1998; Donea and Lindsey, 2005). A sharp blow to the photosphere should excite a broad spectrum of acoustic waves, and the best observations of sunquakes come from frequencies above the p -mode power peak and into the $\sim f^{-2}$ high-frequency variability spectrum of solar emission. Note that observations to date have been limited to image cadences of \approx one minute, corresponding to $f \leq 8.33$ mHz.

The detailed physical mechanism of energy and momentum transfer from the corona into the solar interior remains ill-understood. Three basic mechanisms have been proposed: the essentially hydrodynamic shock-wave heating originating in the chromosphere (Kostiuk and Pikel’ner, 1975; Kosovichev and Zharkova, 1998), the $\mathbf{j} \times \mathbf{B}$ forces from the inevitable magnetic transient (Anwar *et al.*, 1993; Kosovichev and Zharkova, 2001; Sudol and Harvey, 2005; Hudson, Fisher, and Welsch, 2008), and photospheric backwarming (Machado, Emslie, and Avrett, 1989; Martínez-Oliveros, Moradi, and Donea, 2008). The requirement for momentum conservation can in principle help to distinguish among these plausible mechanisms.

The sketch in Figure 1 and the entries in Table 2 show which momentum components could couple well with the solar interior. In the table, the components a , a' , b , and b' are all estimated for the sub-pulse quantities (b' is the reaction to the radiation pressure of the flare continuum emission, not shown in Figure 1). Entries for components c , d are for the entire flare–CME.

From the momentum point of view, within the accuracy of these estimates, the likeliest sources of the seismic wave would be components a or a' (beam or Poynting-flux transport), b (evaporation), or possibly c (the CME). Items a , a' , and b' (radiation pressure) may be excludable because of relatively small momentum transport, but we need better data. Item

d (the draining of the flare-loop system) would be on too long a time scale for the observed seismic waves, and this might be the case for the CME impulse as well. The entry in the table assumes that the entire mass of the CME is accelerated during the impulsive phase, which is certainly an overestimate. Much of the CME mass may come from higher altitudes (e.g., Burkepille *et al.*, 2004) hence requiring long wave-propagation times to couple to the photosphere and a poorer match to the observed frequency range for the seismic waves. The overpressure created by these various impulses (the right-hand column of Table 2) again offers several possibilities, but this overpressure needs to be delivered at or below the photospheric level because of the temporal scales involved (see Figure 2). The ill-understood nature of the CME footprint in the lower solar atmosphere would also be a consideration; it seems likely that the impulse associated with the CME acceleration may press on an extended area of the photosphere, including regions with lower Alfvén speeds.

There is an important caveat regarding chromospheric heating (evaporation) as a source of momentum for seismic waves, as illustrated in Figure 1: the motion of the evaporated mass is arrested by closed fields, which indeed should be in the process of collapsing anyway (Švestka *et al.*, 1987; Hudson, 2000; Wang and Liu, 2010). This impulse tends to counteract the initial impulse of the explosion, producing a negative impulse as described above and shown in Figure 1. The separation between these impulses would be the time scale for the evaporative flow, which is limited by the ion sound speed. Observations at wave frequencies smaller than the inverse of this time scale would not detect so much seismic energy; currently a typical frequency range for seismic observations is 5–7 mHz, which corresponds to a time scale of about 160 seconds. Furthermore, multiple elementary impulses (our example has ten seconds) would tend to overlap and confuse one another (Kosovichev, 2007). Thus we need to regard the momentum inferred from the flare explosion as an upper limit to what could be coupled into the solar interior.

4. Conclusions

The momentum available from flare dynamics appears to be adequate to couple energy into interior seismic waves; within likely uncertainties the momentum could be that associated with the primary energy release from the corona, the overpressure associated with the evaporative flow, or conceivably the CME acceleration. The white-light flare radiation itself contains insufficient momentum, although the backwarming it might induce could suffice in principle (e.g., Moradi *et al.*, 2007). We have noted that the evaporative flow tends to be self-canceling since its motion is arrested, and this action produces an opposite impulse. This would tend to reduce the sunquake amplitudes at lower frequencies, but the time scales would depend on the detailed geometry of the flare. We suggest that an analysis of this impulse could be informative, in the sense that the seismic wave could provide quantitative information about the evaporation process. The time scales are indecisive at present because of the limitations, both inherent and practical, of the wave observations. The exact mechanisms involved with the linkage between solar exterior and solar interior remain unclear, although several plausible schemes have been proposed.

The seismic-wave impulses in principle test our knowledge of the solar interior at its interface with an active region. The coupling of energy between the exterior and the interior, on a specified time scale, depends sensitively on the structure of the atmosphere in the active region (see Figure 2). We may hope that comprehensive observations of the impulsive-phase signatures of solar flares, and their induced seismic waves, can help us to understand flare-induced perturbations of the solar atmosphere.

The requirement for momentum conservation at the point of initial energy release implies that comparable amounts of energy must be lost to sinks other than the chromospheric radiation or evaporation processes. If this momentum is not absorbed by the CME ejection, which could not be the case in a flare without a CME (*e.g.*, Klein, Trotter, and Klassen, 2010), it must be lost into the solar wind and could be detectable eventually by other means. Its presence requires an increase in the total energy of a flare over and above the amounts needed for the flare emission and the CME ejection, as considered in current estimates. It could appear in the lower atmosphere in a form too diffuse to have been detected yet, or more likely it could be hidden in the solar wind.

Acknowledgements This work was supported by NASA under contract NAS 5-98033 for RHESSI. Support at Glasgow came from the EU's SOLAIRE Research and Training Network at the University of Glasgow (MTRN-CT-2006-035484), the EC-funded HESPE project (FP7-2010-SPACE-1-263086), Rolling Grant ST/F002637/1 from the UK's Science and Technology Facilities Council, Leverhulme grant F00-179A, and a Fellowship from the Royal Commission for the Exhibition of 1851 (AR).

References

- Anwar, B., Acton, L.W., Hudson, H.S., Makita, M., McClymont, A.N., Tsuneta, S.: 1993, Rapid sunspot motion during a major solar flare. *Solar Phys.* **147**, 287–303. doi:[10.1007/BF00690719](https://doi.org/10.1007/BF00690719).
- Axford, W.I., McKenzie, J.F.: 1992, The origin of high speed solar wind streams. In: Marsch, E., Schwenn, R. (eds.) *Solar Wind Seven Colloquium*, Pergamon, Oxford, 1–5.
- Belcher, J.W.: 1971, Alfvénic wave pressures and the solar wind. *Astrophys. J.* **168**, 509. doi:[10.1086/151105](https://doi.org/10.1086/151105).
- Birn, J., Fletcher, L., Hesse, M., Neukirch, T.: 2009, Energy release and transfer in solar flares: Simulations of three-dimensional reconnection. *Astrophys. J.* **695**, 1151–1162. doi:[10.1088/0004-637X/695/2/1151](https://doi.org/10.1088/0004-637X/695/2/1151).
- Brown, J.C.: 1971, The deduction of energy spectra of non-thermal electrons in flares from the observed dynamic spectra of hard X-ray bursts. *Solar Phys.* **18**, 489–502. doi:[10.1007/BF00149070](https://doi.org/10.1007/BF00149070).
- Brown, J.C., Craig, I.J.D.: 1984, The importance of particle beam momentum in beam-heated models of solar flares. *Astron. Astrophys.* **130**, L5–L7.
- Burkepile, J.T., Hundhausen, A.J., Stanger, A.L., St. Cyr, O.C., Seiden, J.A.: 2004, Role of projection effects on solar coronal mass ejection properties: I. A study of CMEs associated with limb activity. *J. Geophys. Res.* **109**, A03103. doi:[10.1029/2003JA010149](https://doi.org/10.1029/2003JA010149).
- Canfield, R.C., Metcalf, T.R., Zarro, D.M., Lemen, J.R.: 1990, Momentum balance in four solar flares. *Astrophys. J.* **348**, 333–340. doi:[10.1086/168240](https://doi.org/10.1086/168240).
- Dere, K.P., Brueckner, G.E., Howard, R.A., Koomen, M.J., Korendyke, C.M., Kreplin, R.W., Michels, D.J., Moses, J.D., Moulton, N.E., Socker, D.G., St. Cyr, O.C., Delaboudinière, J.P., Artzner, G.E., Brunaud, J., Gabriel, A.H., Hochedez, J.F., Millier, F., Song, X.Y., Chauvineau, J.P., Marioge, J.P., Defise, J.M., Jamar, C., Rochus, P., Catura, R.C., Lemen, J.R., Gurman, J.B., Neupert, W., Clette, F., Cugnon, P., van Dessel, E.L., Lamy, P.L., Llebaria, A., Schwenn, R., Simnett, G.M.: 1997, EIT and LASCO observations of the initiation of a coronal mass ejection. *Solar Phys.* **175**, 601–612. doi:[10.1023/A:1004907307376](https://doi.org/10.1023/A:1004907307376).
- Donea, A.C., Lindsey, C.: 2005, Seismic emission from the solar flares of 2003 October 28 and 29. *Astrophys. J.* **630**, 1168–1183. doi:[10.1086/432155](https://doi.org/10.1086/432155).
- Emslie, A.G., Dennis, B.R., Holman, G.D., Hudson, H.S.: 2005, Refinements to flare energy estimates: A followup to “Energy partition in two solar flare/CME events” by A.G. Emslie *et al.* *J. Geophys. Res.* **110**, 11103. doi:[10.1029/2005JA011305](https://doi.org/10.1029/2005JA011305).
- Fisher, G.A., Bercik, D.J., Welsch, B.T., Hudson, H.S.: 2011, Momentum balance in eruptive solar flares: The vertical Lorentz force acting on the solar atmosphere and the solar interior. *Solar Phys.*, submitted.
- Fletcher, L., Hudson, H.S.: 2008, Impulsive phase flare energy transport by large-scale Alfvén waves and the electron acceleration problem. *Astrophys. J.* **675**, 1645–1655. doi:[10.1086/527044](https://doi.org/10.1086/527044).
- Fletcher, L., Hannah, I.G., Hudson, H.S., Metcalf, T.R.: 2007, A TRACE white light and RHESSI Hard X-ray study of flare energetics. *Astrophys. J.* **656**, 1187–1196. doi:[10.1086/510446](https://doi.org/10.1086/510446).
- Fontenla, J.M., Curdt, W., Haberreiter, M., Harder, J., Tian, H.: 2009, Semiempirical models of the solar atmosphere. III. Set of non-LTE models for far-ultraviolet/extreme-ultraviolet irradiance computation. *Astrophys. J.* **707**, 482–502. doi:[10.1088/0004-637X/707/1/482](https://doi.org/10.1088/0004-637X/707/1/482).
- Gary, G.A.: 2001, Plasma beta above a solar active region: Rethinking the paradigm. *Solar Phys.* **203**, 71–86.

- Haerendel, G.: 2009, Chromospheric evaporation via Alfvén waves. *Astrophys. J.* **707**, 903–915. doi:[10.1088/0004-637X/707/2/903](https://doi.org/10.1088/0004-637X/707/2/903).
- Hudson, H.S.: 1972, Thick-target processes and white-light flares. *Solar Phys.* **24**, 414–428.
- Hudson, H.S.: 2000, Implosions in coronal transients. *Astrophys. J. Lett.* **531**, L75–L77. doi:[10.1086/312516](https://doi.org/10.1086/312516).
- Hudson, H.S., Cliver, E.W.: 2001, Observing coronal mass ejections without coronagraphs. *J. Geophys. Res.* **106**, 25199–25214. doi:[10.1029/2000JA004026](https://doi.org/10.1029/2000JA004026).
- Hudson, H.S., Webb, D.F.: 1997, Soft X-Ray Signatures of Coronal Ejections. In: Crooker, N., Joselyn, J.A., Feynman, J. (eds.) *Coronal Mass Ejections, Geophys. Monogr.* **99**, 27–38.
- Hudson, H.S., Fisher, G.H., Welsch, B.T.: 2008, Flare energy and magnetic field variations. In: Howe, R., Komm, R.W., Balasubramaniam, K.S., Petrie, G.J.D. (eds.) *Subsurface and Atmospheric Influences on Solar Activity CS-383*, Astron. Soc. Pacific, San Francisco, 221–226.
- Hudson, H.S., Wolfson, C.J., Metcalf, T.R.: 2006, White-light flares: A TRACE/RHESSI overview. *Solar Phys.* **234**, 79–93. doi:[10.1007/s11207-006-0056-y](https://doi.org/10.1007/s11207-006-0056-y).
- Hyder, C.L.: 1967, A phenomenological model for disruptions brusques followed by flarelike chromospheric brightenings, II: Observations in active regions. *Solar Phys.* **2**, 267–284. doi:[10.1007/BF00147842](https://doi.org/10.1007/BF00147842).
- Isobe, H., Kubo, M., Minoshima, T., Ichimoto, K., Katsukawa, Y., Tarbell, T.D., Tsuneta, S., Berger, T.E., Lites, B., Nagata, S., Shimizu, T., Shine, R.A., Suematsu, Y., Title, A.M.: 2007, Flare ribbons observed with G-band and Fe I 6302 Å, filters of the solar optical telescope on board Hinode. *Publ. Astron. Soc. Japan* **59**, S807–S813.
- Kane, S.R., Donnelly, R.F.: 1971, Impulsive hard X-ray and ultraviolet emission during solar flares. *Astrophys. J.* **164**, 151–163. doi:[10.1086/150826](https://doi.org/10.1086/150826).
- Kiplinger, A.L., Dennis, B.R., Frost, K.J., Orwig, L.E.: 1984, Fast variations in high-energy X-rays from solar flares and their constraints on nonthermal models. *Astrophys. J. Lett.* **287**, L105–L108. doi:[10.1086/184408](https://doi.org/10.1086/184408).
- Klein, K., Trotter, G., Klassen, A.: 2010, Energetic particle acceleration and propagation in strong CME-less flares. *Solar Phys.* **263**, 185–208. doi:[10.1007/s11207-010-9540-5](https://doi.org/10.1007/s11207-010-9540-5).
- Knight, J.W., Sturrock, P.A.: 1977, Reverse current in solar flares. *Astrophys. J.* **218**, 306–310. doi:[10.1086/155683](https://doi.org/10.1086/155683).
- Kosovichev, A.G.: 2007, The cause of photospheric and helioseismic responses to solar flares: High-energy electrons or protons? *Astrophys. J. Lett.* **670**, L65–L68. doi:[10.1086/524036](https://doi.org/10.1086/524036).
- Kosovichev, A.G., Zharkova, V.V.: 1998, X-ray flare sparks quake inside Sun. *Nature* **393**, 317–318. doi:[10.1038/30629](https://doi.org/10.1038/30629).
- Kosovichev, A.G., Zharkova, V.V.: 2001, Magnetic energy release and transients in the solar flare of 2000 July 14. *Astrophys. J. Lett.* **550**, L105–L108. doi:[10.1086/319484](https://doi.org/10.1086/319484).
- Kostiuk, N.D., Pikel'ner, S.B.: 1975, Gasdynamics of a flare region heated by a stream of high-velocity electrons. *Sov. Astron.* **18**, 590–599.
- Machado, M.E., Emslie, A.G., Avrett, E.H.: 1989, Radiative backwarming in white-light flares. *Solar Phys.* **124**, 303–317. doi:[10.1007/BF00156272](https://doi.org/10.1007/BF00156272).
- Martínez-Oliveros, J.C., Moradi, H., Donea, A.: 2008, Seismic emissions from a highly impulsive M6.7 solar flare. *Solar Phys.* **251**, 613–626. doi:[10.1007/s11207-008-9122-y](https://doi.org/10.1007/s11207-008-9122-y).
- Mauas, P.J.D., Machado, M.E., Avrett, E.H.: 1990, The white-light flare of 1982 June 15—models. *Astrophys. J.* **360**, 715–726. doi:[10.1086/169157](https://doi.org/10.1086/169157).
- McClymont, A.N., Canfield, R.C.: 1984, The unimportance of beam momentum in electron-heated models of solar flares. *Astron. Astrophys.* **136**, L1–L4.
- Milligan, R.O., Dennis, B.R.: 2009, Velocity characteristics of evaporated plasma using Hinode/EUV imaging spectrometer. *Astrophys. J.* **699**, 968–975. doi:[10.1088/0004-637X/699/2/968](https://doi.org/10.1088/0004-637X/699/2/968).
- Moradi, H., Donea, A., Lindsey, C., Besliu-Ionescu, D., Cally, P.S.: 2007, Helioseismic analysis of the solar flare-induced sunquake of 2005 January 15. *Mon. Not. Roy. Astron. Soc.* **374**, 1155–1163. doi:[10.1111/j.1365-2966.2006.11234.x](https://doi.org/10.1111/j.1365-2966.2006.11234.x).
- Najita, K., Orrall, F.Q.: 1970, White light events as photospheric flares. *Solar Phys.* **15**, 176–194.
- Simnett, G.M., Haines, M.G.: 1993, On the production of hard X-rays in solar flares. *Solar Phys.* **130**, 253–263.
- Song, Y., Lysak, R.L.: 1994, Alfvénion, driven reconnection and the direct generation of the field-aligned current. *Geophys. Res. Lett.* **21**, 1755–1758. doi:[10.1029/94GL01327](https://doi.org/10.1029/94GL01327).
- Sudol, J.J., Harvey, J.W.: 2005, Longitudinal magnetic field changes accompanying solar flares. *Astrophys. J.* **635**, 647–658. doi:[10.1086/497361](https://doi.org/10.1086/497361).
- Temmer, M., Veronig, A.M., Vršnak, B., Rybák, J., Gömöry, P., Stoiser, S., Maričić, D.: 2008, Acceleration in fast halo CMEs and synchronized flare HXR bursts. *Astrophys. J. Lett.* **673**, L95–L98. doi:[10.1086/527414](https://doi.org/10.1086/527414).

- Švestka, Z.F., Fontenla, J.M., Machado, M.E., Martin, S.F., Neidig, D.F.: 1987, Multi-thermal observations of newly formed loops in a dynamic flare. *Solar Phys.* **108**, 237–250. doi:[10.1007/BF00214164](https://doi.org/10.1007/BF00214164).
- Švestka, Z.: 1970, The phase of particle acceleration in the flare development. *Solar Phys.* **13**, 471–489.
- Vršnak, B., Lulić, S.: 2000, Formation of coronal Mhd shock waves – I. The basic mechanism. *Solar Phys.* **196**, 157–180.
- Wang, H., Liu, C.: 2010, Observational evidence of back reaction on the solar surface associated with coronal magnetic restructuring in solar eruptions. *Astrophys. J. Lett.* **716**, L195–L199. doi:[10.1088/2041-8205/716/2/L195](https://doi.org/10.1088/2041-8205/716/2/L195).
- Wang, Y., Zhang, J.: 2007, A comparative study between eruptive X-class flares associated with coronal mass ejections and confined X-class flares. *Astrophys. J.* **665**, 1428–1438. doi:[10.1086/519765](https://doi.org/10.1086/519765).
- Wolff, C.L.: 1972, Free oscillations of the Sun and their possible stimulation by solar flares. *Astrophys. J.* **176**, 833–842. doi:[10.1086/151680](https://doi.org/10.1086/151680).
- Yashiro, S., Gopalswamy, N., Akiyama, S., Michalek, G., Howard, R.A.: 2005, Visibility of coronal mass ejections as a function of flare location and intensity. *J. Geophys. Res.* **110**, A12S051–A12S0511. doi:[10.1029/2005JA011151](https://doi.org/10.1029/2005JA011151).
- Zarro, D.M., Canfield, R.C., Metcalf, T.R., Strong, K.T.: 1988, Explosive plasma flows in a solar flare. *Astrophys. J.* **324**, 582–589. doi:[10.1086/165919](https://doi.org/10.1086/165919).
- Zarro, D.M., Sterling, A.C., Thompson, B.J., Hudson, H.S., Nitta, N.: 1999, SOHO EIT observations of extreme-ultraviolet “Dimming” associated with a halo coronal mass ejection. *Astrophys. J. Lett.* **520**, L139–L142. doi:[10.1086/312150](https://doi.org/10.1086/312150).
- Zhang, J., Dere, K.P., Howard, R.A., Vourlidas, A.: 2004, A study of the kinematic evolution of coronal mass ejections. *Astrophys. J.* **604**, 420–432. doi:[10.1086/381725](https://doi.org/10.1086/381725).
- Zharkova, V.V.: 2008, The mechanisms of particle kinetics and dynamics leading to seismic emission and sunquakes. *Solar Phys.* **251**, 665–666. doi:[10.1007/s11207-008-9266-9](https://doi.org/10.1007/s11207-008-9266-9).
- Zharkova, V.V., Zharkov, S.I.: 2007, On the origin of three seismic sources in the proton-rich flare of 2003 October 28. *Astrophys. J.* **664**, 573–585. doi:[10.1086/518731](https://doi.org/10.1086/518731).